NASA

Technical Memorandum 80574

# Ocean Chlorophyll Studies From a U-2 Aircraft Platform



H. H. Kim, C. R. McClain, L. R. Blaine, W. D. Hart, L. P. Atkinson, and J. A. Yoder

AUGUST 1979

National Aeronautics and
Space Administration

**Goddard Space Flight Center**
Greenbelt, Maryland 20771

TM 80574

# OCEAN CHLOROPHYLL STUDIES FROM A U-2 AIRCRAFT PLATFORM

By

Hongsuk H. Kim
Charles R. McClain
Lamdin R. Blaine
William D. Hart†
Larry P. Atkinson*
and
James A. Yoder*

August 1979

GODDARD SPACE FLIGHT CENTER
Greenbelt, Maryland 20771

---

†The author is with Science Systems and Applications, Inc., Lanham, MD.
*The authors are with Skidaway Institute of Oceanography, Savannah, GA.

## CONTENTS



## LIST OF TABLES



## LIST OF ILLUSTRATIONS

# OCEAN CHLOROPHYLL STUDIES FROM A U-2 AIRCRAFT PLATFORM

By
Hongsuk H. Kim, Charles R. McClain,
Lamdin R. Blaine, William D. Hart†
Larry P. Atkinson* and James A. Yoder*

## ABSTRACT

Chlorophyll gradient maps of large ocean areas were generated from U2/OCS data obtained over test sites in the Pacific and Atlantic Oceans. The delineation of oceanic features using the upward radiant intensity relies on an analysis method which presupposes that radiation backscattered from the atmosphere and ocean surface can be properly modeled using a measurement made at 778 nm. The calculation of atmospheric radiance was performed using a method developed by J. V. Dave. An estimation of the chlorophyll concentration is performed by properly ratioing radiances measured at 472 nm and 548 nm after removing the atmospheric effects. The correlation between the remotely sensed data and in-situ surface chlorophyll measurements has been validated in two sets of data. The results show that the correlation between the in-situ measured chlorophyll and the derived quantity is a negative exponential function and the correlation coefficient was calculated to be -0.965.

---

†The author is with Science Systems and Applications, Inc., Lanham, MD.
*The authors are with Skidaway Institute of Oceanography, Savannah, GA.

# OCEAN CHLOROPHYLL STUDIES FROM A U-2 AIRCRAFT PLATFORM

## INTRODUCTION

During the last two decades, the space program has given us the opportunity to view the ocean from a high altitude platform. As a result, interesting applications of remote sensing technology have emerged, one of which is the monitoring of chlorophyll pigments in the open ocean. Chlorophyll information is directly related to marine productivity, thus providing the capability of detecting locations of high biological activity. Development of operational systems which provide this information should have tremendous benefits for the harvesting and maintenance of viable fisheries. Also, it would be extremely valuable when coupled with sea surface temperature for the oceanographic community involved in basic research.

In 1969, Clark *et al.*, were the first investigators to measure upwelling light from an aircraft at relatively low altitudes while simultaneously obtaining measurements of chlorophyll concentrations from a surface vessel, [Clark *et al.*, 1970]. Based on their initial success, NASA/GSFC in 1974 began a sensor study directed toward the development of an ocean color scanner (OCS). However, the complexities associated with the sensor development and data analysis techniques have necessarily delayed publication of quantitative results. For instance, from the results of Clark, *et al.* and later U-2 high altitude flights, it became apparent that the development of reliable quantitative estimates of surface chlorophyll required that the contribution of backscattered radiation from the atmosphere and sea surface had to be removed from the total upwelling radiance [Hovis *et al.*, 1973]. In ensuing years, numerous field and theoretical works have been performed in an attempt to understand the various atmospheric and oceanic properties which determine the interactions between sunlight, the atmosphere and the ocean. Although knowledge of radiative transfer in the atmosphere and especially the hydrosphere remains incomplete, it now appears

that sufficient progress has been made to enable us to provide data products useful to the oceanographic community. By far the most ambitious effort towards realization of this goal is the Nimbus-7/Coastal Zone Color Scanner which was launched in August, 1978.

In this paper, a recent OCS study is described which was initiated to prepare for a future space experiment, i.e., the space shuttle ocean color experiment scheduled for launch in 1980. In the following sections, the aircraft sensor application effort, from the instrumentation to a recently successful field mission will be discussed, emphasizing the various scientific aspects which underlie this remote sensing technology. This particular exercise was a coordinated effort with a team of oceanographers who are studying interactions between the Gulf Stream and adjacent shelf waters in the South Atlantic Bight.

## U-2 OCEAN COLOR SCANNER (OCS)

A prototype OCS was built by NASA/GSFC to be mounted on a U-2/aircraft which operates at 20 km. Later two additional units were built with slight modifications so that the second unit can be mounted on a Lear Jet which flies at an altitude of 10 km and the third on the Space Shuttle which will be operated at an altitude of 280 km in 1980. The U-2/OCS is a 10-channel scanning radiometer having a 90 degree total field-of-view and a 3.5 milliradian instantaneous-field-of-view (IFOV). The general instrument and platform parameters are given in Table 1. The critical

Table 1
OCS and U2 Parameters

| | |
|---|---|
| Aircraft Speed | 201 meter/sec (390 knots nominal) |
| Aircraft Altitude | 19.8 kilometers (nominal) |
| Angular Resolution (IFOV) | 3.5 mr |
| Footprint | 69.3 m x 69.3 m |
| FOV | ±45° from nadir |
| Scan Rate (mirror speed) | 2.727 revolutions/sec |
| Swath Width | 39.6 kilometers |
| Output Voltage | 0 volts to ±5 volts |
| Output Bandwidth | 0 to 2500 Hertz |
| Output rms Noise Level | 8 millivolts (nominal) |

radiometric and spectral characteristics i.e., spectral band, center wavelength, bandwidth, and signal-to-noise ratio are given in Table 2.

When flown on the U-2 aircraft the OCS swath width is 39.6 km and the footprint at nadir is approximately (69 meters)$^2$. For comparison the footprint of the Nimbus-7 CZCS is (826 meters)$^2$.

The scanner utilizes a fully rotating scan mirror turning at the rate of 2.727 revolutions per second and viewing the earth through scan angles of ±45 degrees from nadir. From the primary scanning mirror, the incoming radiation is reflected into an optical system which includes a Dall-Kirkham telescope, an optical disperser, a fiber optic receiver, and a cluster of ten silicon diode detectors. The dispersing unit consists of a 600 line per mm plane diffraction grating, and an image receiving head composed of 24 fiber optics windows. The fiber optics receiver is adjustable along the exit focal plane so that one of the 24 windows can be centered on a selected spectral channel. Physically the instrument package can be described as a cylinder 75 cm long by 27 cm in diameter and weighing about 30 kgms. Because of the scan mirror and the grating element in the optical train, the instrument is sensitive to the polarization of incoming light.

The change in signal output for parallel and perpendicular polarization components are about 20 percent against a totally polarized light source. It has been estimated that this 20 percent degree

Table 2
Optical Parameters of the U-2 Ocean Color Scanner Channels

| Channel | Center Wavelength (nm) | Full Bandwidth at Half Intensity (nm) | Spectral Radiance (Ocean Targets) mw/cm$^2$ sr $\mu$m | Calibration Function Slope $\frac{\text{mw cm}^{-2}\ \text{sr}^{-1}\ \mu\text{m}}{\text{volt}}$ |
|---|---|---|---|---|
| 1 | 431 | 24.2 | 25.54 | 7.298 |
| 2 | 472 | 26.0 | 20.94 | 5.984 |
| 3 | 506 | 25.0 | 13.49 | 3.853 |
| 4 | 548 | 26.3 | 8.276 | 2.365 |
| 5 | 586 | 24.1 | 6.334 | 1.810 |
| 6 | 625 | 25.3 | 5.007 | 1.430 |
| 7 | 667 | 24.2 | 3.883 | 1.110 |
| 8 | 707 | 26.0 | 3.167 | 0.9049 |
| 9 | 738 | 24.0 | 40.33 | 11.52 |
| 10 | 778 | 26.1 | 2.146 | 0.6131 |

of polarization sensitivity in all spectral channels will introduce a small error from polarized sky light, i.e., an error in the range of few percent in intensity measurement will occur in the blue channels under a Raleigh Sky if the sensor is flown in the solar radiant plane (Appendix A). This trait of the U-2/OCS has been recognized and the effects are minimized by flying parallel to the solar radiant plane.

U-2/OCS flight data are distributed to several investigators in the US and Western European nations. In order to assure the radiometric accuracy of the instrument, approximately every 6 months the OCS is brought back to the laboratory for testing and calibration checks. The inspection consists of an examination of each channel with respect to its spectral position, half width, shape and radiometric calibration. The spectral examination is carried out using a 0.5 meter Ebert spectrometer and the radiometric phase using a 1.83 meter (6 foot) integrating sphere which is color corrected to approximate the sun's spectral power distribution. With respect to the radiometric calibration, the instrument scans the sphere's exit port and output from each channel is adjusted to give maximum signal (5.0 volts) when the expected ocean color radiance is viewed by the sensor.

The principle of the integrating sphere was proposed by Sumphner [1892]. He showed that if an illumination source is placed inside a hollow sphere which is covered internally with a perfectly diffusing surface, the generated luminance is lambertian and is directly proportional to the total flux emitted by the source. At GSFC, a 1.83 meter (6 ft.) diameter integrating sphere containing twelve 200 watt lamps with a 30 mm diameter port is used to simulate the upwelling light over the ocean. The inside of the sphere is coated with barium sulphate, which acts as a diffusing medium.

The integrating sphere is calibrated using a spectrally calibrated quartz iodide secondary standard lamp. The National Bureau of Standards (NBS) provides this lamp together with measurements of its flux at 35 wavelengths in the 0.25 to 1.6 micrometer range. A spectrally calibrated monochromater views both the standard lamp and the sphere to be calibrated through a 40 cm intermediate integrating sphere. This intermediate sphere is secured at the entrance slit of the monochromater and can view both sources at all 35 calibrated wavelengths. The ratio of reflections at each wavelength is the ratio of the flux intensities. Since the flux of the standard is known, the

flux from the sphere can be determined at these 35 points and interpolated for the remaining wavelengths. This procedure is repeated for illuminations of 12 lamps down to one lamp inside the sphere. The longterm stability of the large sphere is about 5 percent. The OCS instruments are calibrated frequently, and are maintained within a 2 percent fluctuation limit to the sphere reading.

In addition to the aforementioned calibration, the performance of the scanner was also evaluated using sky radiance. To effect such a comparison, the downwelling intensity was measured at ground level by pointing the OCS toward the zenith and the resulting measurements were corrected to spectral radiance values and compared with numerically calculated values. In Figure 1, a comparison of the U-2/OCS measurements with the calculated downward radiance at sea level for a clear atmosphere is shown. In the figure, the intensities measured by the OCS, in triangular points, are compared with a theoretical spectral curve which is shown by dots and the dotted line. The spectral characteristics of the downwelling intensities are almost defined for given atmospheric conditions by the sun's position, $\theta s$, the ground reflectivity, $\rho$, and the aerosol content in the atmosphere. Especially, the blueness of the sky, or the variation of the intensity of the sky radiation, is largely influenced by the amount of aerosol present. As shown in the figure, the majority of the measured points overlap the theoretical spectral curve for a given $\tau_{Mie}$. This can be interpreted as an indication of the instrument's reliability.

The calculation of the downwelling radiance was performed using a plane parallel model of the atmosphere which was originally developed by J. V. Dave [1972]. Values of the solar irradiance constants ($F_\lambda^0$ in $W/m^{-2}$ $-\mu$) used to compute the absolute radiance at the OCS wavelengths were taken from Thekaekara's Table [Thekaekara, 1974].

## FIELD EXPERIMENTS

The U-2/OCS and two other replicas have been frequently flown to study the oceans surrounding continental North America and Western Europe. These flights were performed in support of various ocean studies. Some of the ocean features being observed were quite visible even at

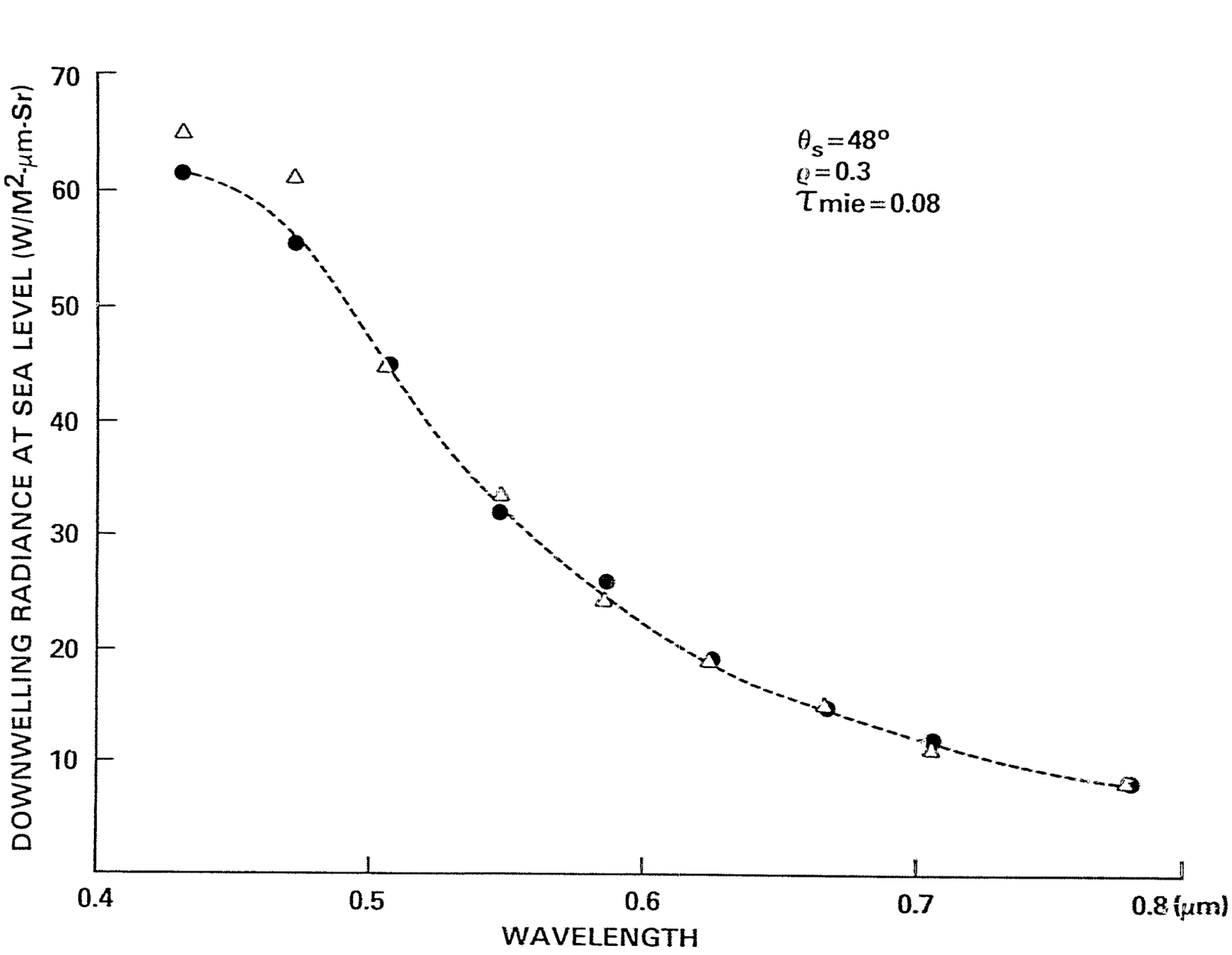


Figure 1. A Measurement of Downward Atmospheric Radiance by the Use of U2/OCS, in Triangle Points, Is Compared with the Calculated Values Given in Circles.

raw data form, i.e., quick look analog tape images of acid dumps in the New York Bight and Red Tide (Gymnodiniums Brevi) blooms in the Gulf of Mexico. However in the cases presented here the chlorophyll feature was not immediately visible in raw data form and additional image enhancement processing accompanied by the atmospheric effects correction was needed to bring out the feature.

In the early stages of the OCS project, it became apparent that extraction of the chlorophyll signature from field data was exceedingly complicated and in some cases, it was totally impossible due to the extenuating extrinsic factors influencing the ocean radiance measurement.

Therefore, it was necessary to develop a coherent analysis technique applicable to interpret data obtained under a set of appropriate weather and ocean conditions. Therefore, recent U-2/OCS flights were set to view the oceans according to the following rules:

a. First, the OCS data were taken only over the deep and clear water of the open ocean. It has been observed that the reflection of light from the ocean floor and scattering by sediment would strongly interfere with the chlorophyll absorption signature. A reliable method of treating underwater radiative transfer processes for turbid ocean water is not well established as of this writing. Until one can specify the light scattering properties of various phytoplankton and marines sediments with arbitrary size distribution, only the open ocean color with relatively few impurities under a near Rayleigh sky is dealt with in the present analysis.

b. Secondly, care was taken to collect overflight data totally free from sun-glint on the ocean surface. The sun-glint from the ocean surface is a substantial effect that will obliterate any information about the content of the subsurface phenomena. Even though the nature of sun-glint and its propagation patterns on airborne imagery are well understood, [Cox and Munk, 1956 and Plass *et al.*, 1976] the removal of its effects from ocean color data usually do not allow the isolation of true water radiance from others. Therefore, it was determined that glint must be avoided by flying the aircraft directly toward or away from the sun and, at the same time, maintaining a solar zenith angle within a range of 35-60 degrees for optimum conditions.

c. In order to minimize the atmospheric effects, the data were taken only when the sky was clear and the surface of the ocean was relatively free of white caps.

d. Lastly, overflight data became useful only when supporting sea truth was properly collected. The ocean chlorophyll distribution can be a rapidly changing phenomena depending on the particular oceanic system being studied and variability encompasses not only horizontal but also vertical patterns. In order to establish the quantative relation of remotely sensed data with nature, the in-situ measurements should be made at a precise location within a few hours of the time of the overflight. Since the U-2/OCS pixel size is on the order of $(69\ m)^2$, the ship's absolute position must be known within a hundredth of a minute. Chlorophyll concentration and other pertinent ocean data must be taken at the surface and at several depths to give a vertical profile as well as a large area horizontal distribution pattern.

The shipborne surface truth gathering activity is the most important and difficult requirement to meet in practice. It has taken several years to generate an ideal flight data set and to repeat similar experiments to verify the initial success. The first successful data were obtained during the Monterey Bay Biological Experiment which was performed in May and September of 1977. An opportunity for a second open ocean chlorophyll experiment did not materialize until a pre-Georgia Bight Experiment (GABEX) took place off the coast of Jacksonville, Florida, in the Spring of 1979.

## ATMOSPHERIC EFFECTS CORRECTION

Essentially, the upwelling radiance measured at the high altitude aircraft platform consists of two primary components, namely:

a. Photons that have not penetrated the sea surface but are returned to the sensor from the atmospheric path and sea surface backscattering. The effects of these photons are considered to be extrinsic to the ocean color.

b. The photons that indeed penetrated the sea surface and whose signatures are associated with the water and its chlorophyll concentration.

The upwelling intensity in the visible channel, $I_{\lambda_i}^{Total}$, can be expressed as:

$$I_{\lambda_i}^{Total} = I_{\lambda_i}^{Atm\ \&\ Sfc} + I_{\lambda_i}^{Water} \qquad (1)$$

Separating these two components, the $I_{\lambda_i}^{Water}$ from the $I_{\lambda_j}^{Atm\ \&\ Sfc}$ is difficult. In practice the up- and downwelling intensity of the sun and diffused skylight is frequently measured by surface crews using radiometers. However no such measurements were taken during the OCS flight in Spring, 1979.

As an alternate approach, the use of the upwelling radiance in the near infrared channel for estimating atmospheric effects was proposed earlier and has been studied recently [Gordon, 1978]. Ocean water is nearly opaque to near infrared radiation and the upwelling intensity in the infrared region, $I_{\lambda_j}^{Total}$, is simply,

$$I_{\lambda_j}^{Total} = I_{\lambda_j}^{Atm\ \&\ Sfc} \text{ (as } I_{\lambda_j}^{Water} \text{ is small)} \tag{2}$$

By modeling the upwelling radiances in both the visible and near-infrared regions, one can derive a proportionality constant, $\eta_{\lambda_{ij}}$. This constant can then be applied to observations on a pixel by pixel basis, to correct the atmospheric perturbations imposed upon the visible radiation. We have:

$$\eta_{\lambda_{ij}} = \frac{I_{\lambda_i}^{Atm\ \&\ Sfc}}{I_{\lambda_j}^{Atm\ \&\ Sfc}} \tag{3}$$

Then the true water radiance (or subsurface radiance) term at each pixel can be obtained by:

$$I_{\lambda_i}^{Water} = I_{\lambda_i}^{Total\ Measured} - \eta_{\lambda_{ij}} \cdot I_{\lambda_j}^{Total\ Measured} \tag{4}$$

The method defined in equation (4) is essentially an inversion analysis technique, in which the ocean radiance and its wavelength dependence are derived from the measured total upward radiance and the calculated atmospheric radiance. This method assumes well defined radiance values for the atmospheric contribution.

While several numerical methods exist for the calculation of radiation transfer in the atmosphere, modeling of the upwelling radiance was carried out by using a proven method developed by J. V. Dave. In his method, the radiative transfer equation for a given atmosphere model is solved by decomposing it into a series of mutually independent integro-differential equations.

Each of these equations is then solved by dividing the atmosphere into a finite number of layers and using a Gauss-Seidel iterative procedure. The method can be used to compute the intensity of upwelling radiation in an atmosphere bounded at the bottom by a sea surface of assumed reflectivity (Appendix B).

In order to apply this ocean-atmosphere radiance computation method, the conditions under which the data were taken must be scrutinized and correct physical parameters must be incorporated into the transfer equations. The following parameters must be incorporated into the calculations:

a. the solar zenith angle

b. sea surface reflectivity

c. the optical thickness of the atmosphere, refractive index and size distribution of the aerosols. These define the aerosol single-scattering phase function.

Using the Dave method computer programs, one can generate radiation data points for an extensive assortment of atmospheric models. These solutions can then be specifically applied to the particular ocean scene under investigation.

In our analysis, the computation of $\eta_{\lambda_{ij}}$ was performed only for the nadir observation point ($\mu = 1$) and for an altitude of 19.8 km at each of the OCS channels. The aerosol single scattering phase function was calculated using Mie theory assuming a Jungean distribution with $\upsilon^*$ values of 3.2 and 3.5.

Also for convenience, the real component of the aerosol refractive index was assumed to be $M_r$ = 1.50 and the imaginary part, $N_m$, was set at zero. The reflectivity of the ocean was assumed to be 1 percent even though the nominal Fresnel reflectivity of the air-sea interface is 2 percent. The ocean surface reflection is never fully Lambertian, but it is assumed so in the Dave programs. Therefore, in the absence of direct sun-glint into the scanner field-of-view, the ocean surface reflectivity can be assumed much less than 2 percent.

A graphical plot showing the upwelling intensity in each of the Ocean Color Scanner channels as a function of aerosol content for size parameters $\upsilon^*$ = 3.2 and 3.5 is shown in Figure 2. The plots are

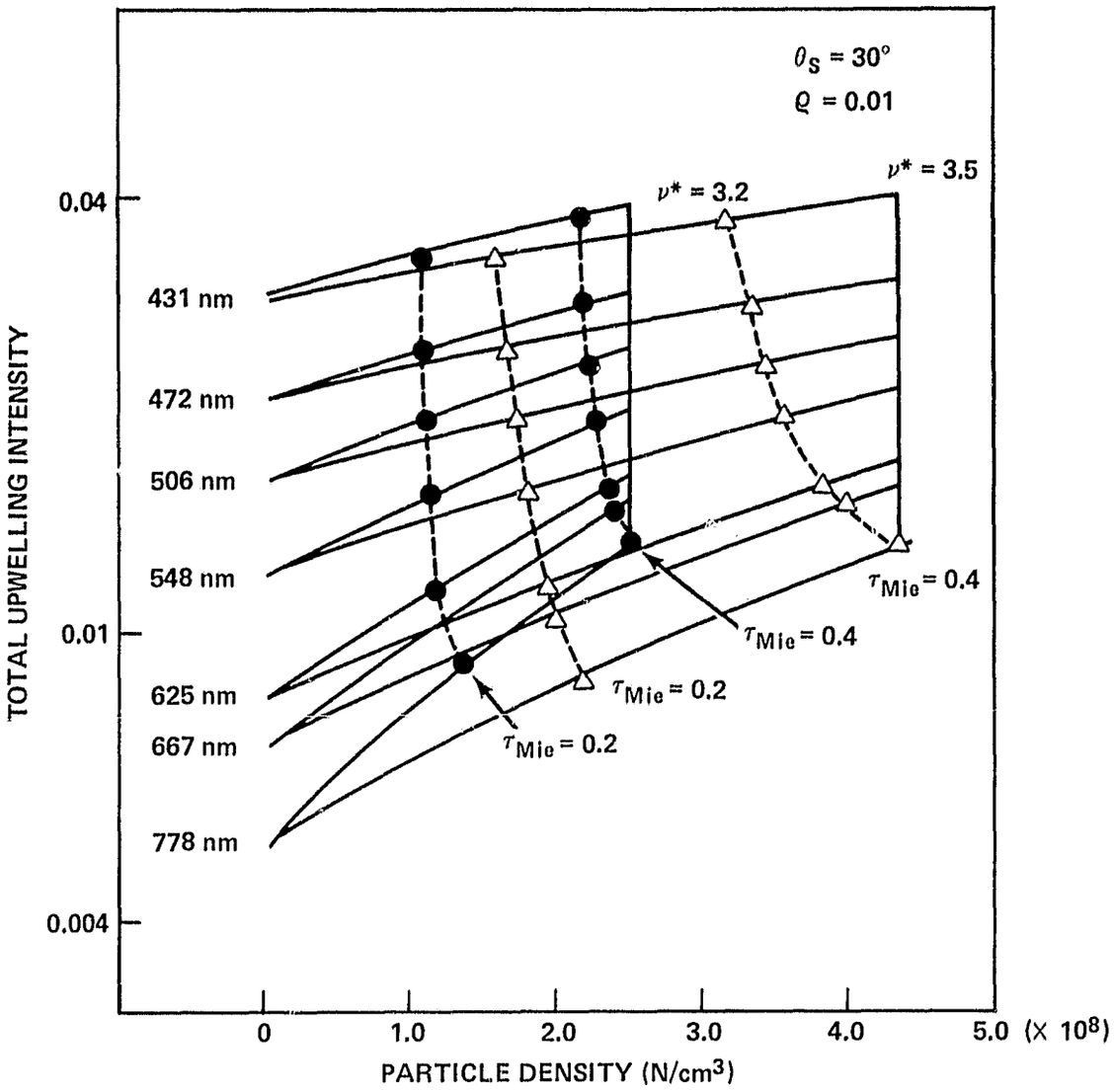


Figure 2. Upwelling Intensity for Each OCS Channel Is Plotted Against Aerosol Content Showing Radiance Differences Due to the Aerosol Size Distributions, $\upsilon^*$ = 3.2 and 3.5. The Calculations Are for Nadir Viewing Normalized to a Solar Zenith Angle of 30° and Ground Reflectivity of 1%.

for a solar zenith angle of 30 degrees and the ordinate intensities were calculated using unity as the value of solar flux at 80 km above the earth's surface.

The parameter $\eta_{\lambda_{ij}}$ from Figure 2 in the following manner. After selecting the appropriate size parameter which is assumed to be applicable to the particular scene being analyzed, the upward intensity for 778 nm is read from the graph for the effective $\tau_{Mie}$ of the scene. The effective $\tau_{Mie}$

defines the aerosol load of the atmosphere. Then the upward atmospheric intensities, $I_{\lambda_j}^{\text{Atm \& Sfc}}$, of the other channels can be read from the graph for this aerosol load corresponding to the $\tau_{\text{Mie}}$. The parameter, $\eta_{\lambda_{ij}}$ for each channel is then determined from equation (3). The curved lines in the figure represent the iso-lines of constant optical thickness. The lines show that wavelength dependency of $\tau_{\text{Mie}}$ for each size distribution $\upsilon^{\lambda}$ = 3.2 in circles and 3.5 in triangles.

From the figure, it can be seen that the error depends strongly on the estimation of the optical thickness at 778 nm and on the assumptions one has to make about the size parameters of the aerosols. In order to minimize the error of estimating the $\tau_{\text{Mie}}$ at 778 nm, a high gain broadband IR channel with a better signal-to-noise performance will be desirable for future systems. The error in approximating the size distribution of the aerosols in the atmosphere may be decreased by an interpolative readout method and knowing the size parameter. A method to empirically derive the Junge parameter from Angstrom's wavelength exponent formula has been discussed in earlier work [Kim *et al.*, 1979].

## DERIVATION OF THE WATER RADIANCE FROM OCS DATA

The color of the ocean is truly diverse, almost any color of the spectrum can be observed from the ocean under appropriate conditions. That means there will be differences in absolute spectral radiance measured from one place to another depending on atmospheric conditions, water depth, its content and sea state.

We have observed many different curves of spectral radiance for various locations. From these circumstances, our experimental studies have been narrowed down to the albedo of the open ocean where the absorption of blue light by the chlorophyll will shift the pure blueness to a somewhat greenish color. Typical absolute spectral radiance of the open ocean should have curves which climb almost monotonically from the near infrared into the blue where the maximum radiance occurs at 430 $\mu$m. It should be noted that typical upwelling spectra from turbid water in the coastal zones should have pronounced differences in the middle wavelength regions of the visible spectrum between 500 nm and 650 nm.

Therefore the OCS flight data was carefully examined to see if the water radiance is affected by variations in hydrosols or bottom reflectance. Only those spectral curves which were obtained at nadir in the absence of any noticeable sun-glint, were considered as true ocean color.

In Figure 3, curves representing absolute spectral radiance produced by total upwelling from the ocean and the atmosphere are shown. The bars in the figure represent the actual measured radiance of nine OCS channels showing the range of values for 2500 pixels taken at the nadir look angle. The original data were taken at the Gulf Stream front off Jacksonville, Florida. Water depths varied from 40 to 200 meters and the data was taken in midafternoon on an essentially clear day.

The measured upwelling spectral radiance at 778 nm was about 4.8 $w/m^2$-$\mu$m-sr and this figure corresponds to a surface albedo of 0.01 according to our clear sky radiance model. Therefore, the upwelling intensity calculations for all wavelengths were performed for a one percent surface reflectivity. The results of the computations of $I_{\lambda i}^{Atm\ \&\ Sfc}$, are shown by triangles and solid lines in the figure. In order to locate a theoretical spectral curve which closely matches with the OCS measurement bars in the figure, the water radiance was added to the surface reflectivity already given as one percent. We assumed the clear ocean radiance model given by Kattawar & Humphreys [1976]. Clark *et al.*, has also shown similar empirical spectral features in their original ocean color work. The outcome of our computations, using albedo slope given by the solid line in Figure 4, is shown by the dotted line in Figure 3. This maneuver is necessary to confirm the validity of the assumptions being made to construct a clear ocean radiance model.

Once the shape of the spectral plot of ocean radiance has been identified, equation (4) can be applied on a pixel by pixel basis. The resultant spectral features of true water radiance at high and low chlorophyll concentrations are given in Figure 5. These spectral features are different from those of the true natural upwellings recorded at the immediate surface. Instead they represent the water radiance that can be perceived at a 20 km height. The top trace belongs to the upwelling radiance of the ocean area where the chlorophyll concentration was reported as 0.2 $\mu$g/L at a 2 meter depth and the corresponding chlorophyll value of the lower trace was 7 $\mu$g/L respectively. Interestingly the

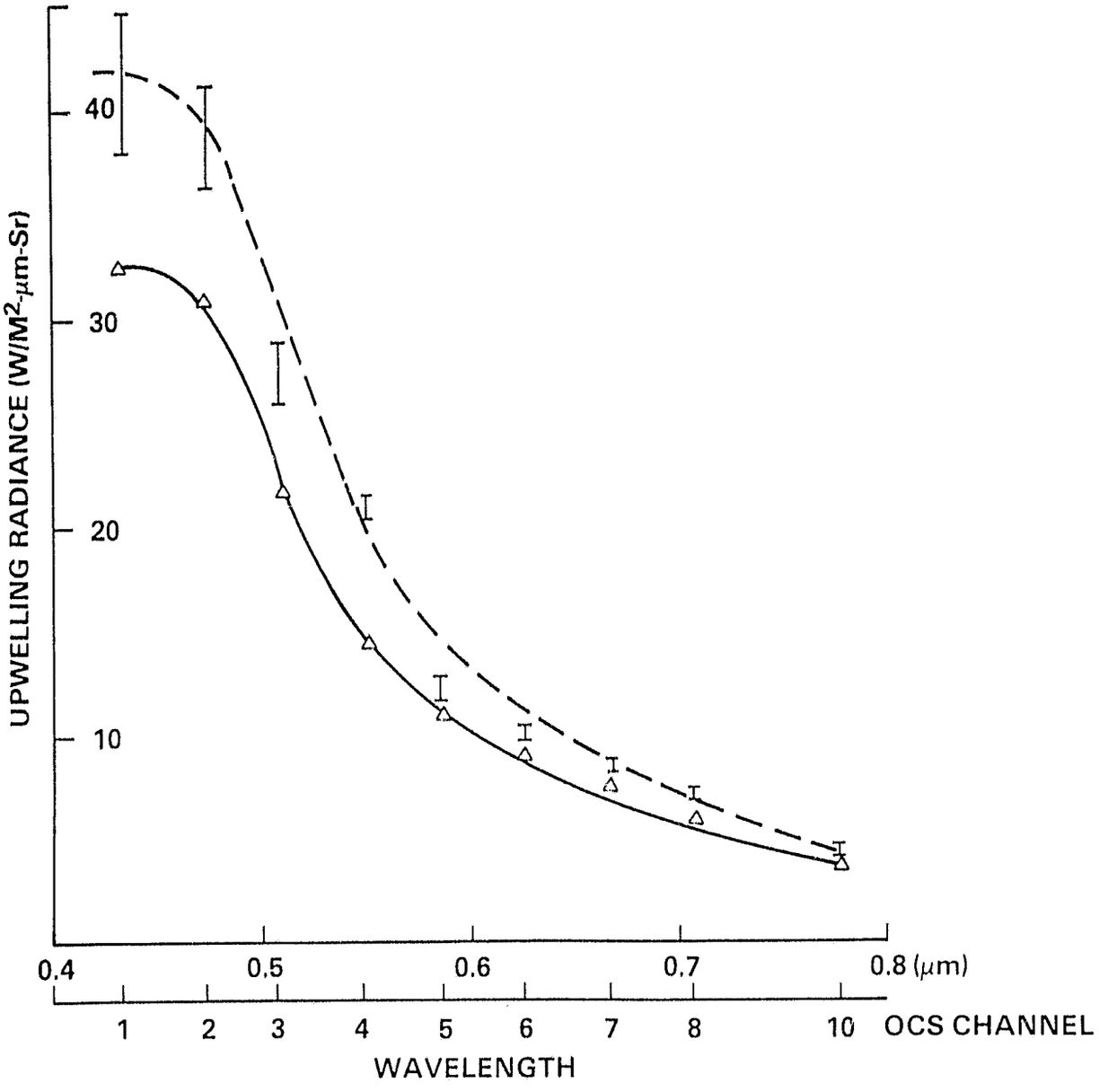


Figure 3. Plots of Upwelling Radiance at Nine OCS Channels. Bars Are Actual OCS Data Taken from U-2 Flight off the Jacksonville, Florida. The Solid Line Indicates Calculated Radiance of the Atmosphere and Surface Reflection, and the Dotted Line Corresponds to Calculated Radiance Which Includes the Radiance Contribution of Ocean Subsurface Layer.

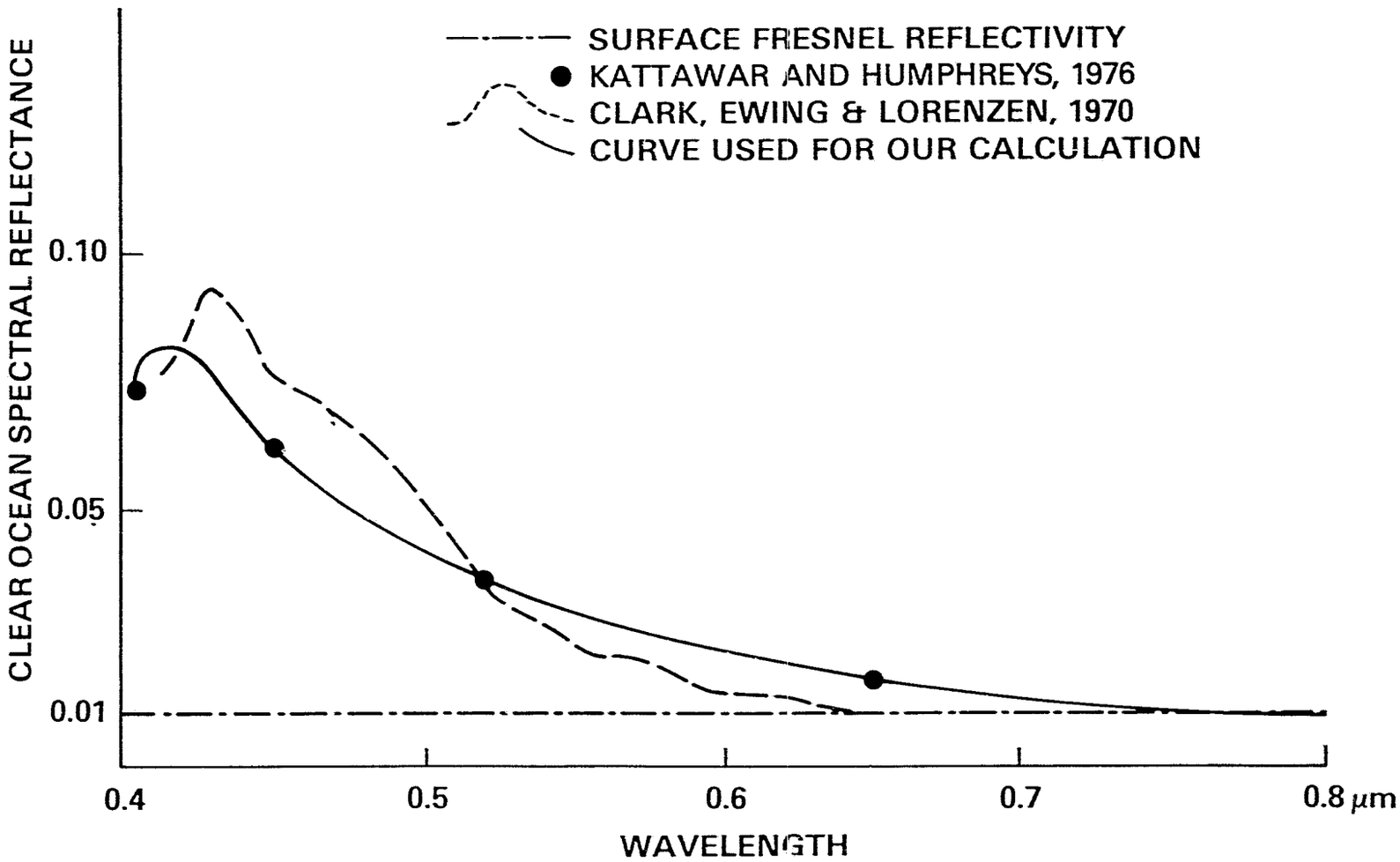


Figure 4. Plots of Clear Ocean Albedo Showing Their Wavelength Dependency. Solid Line Profile Was Used for Our Calculation.

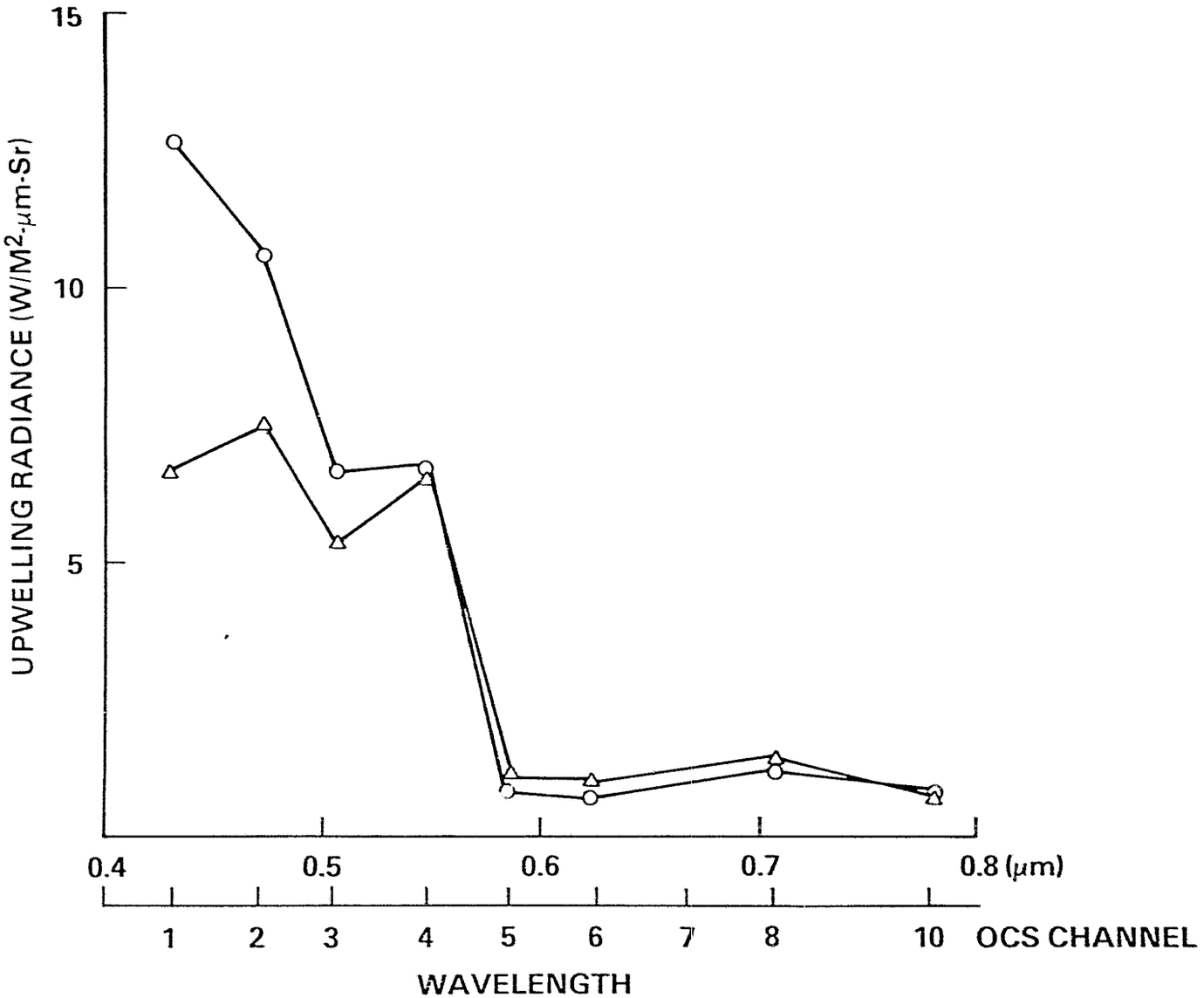


Figure 5. Derived Water Radiance from OCS Data: The Spectral Feature from Low Chlorophyll Concentration Is Shown in Dots and Interconnecting Line. The Triangular Trace Belongs to that of a High Chlorophyll Zone.

curves in Figure 5 resemble the theoretical water radiance plots, minus the white cap contributions, given by Quenzel *et al.* [1978].

## CHLOROPHYLL ANALYSIS AND VALIDATION OF THE RESULTS WITH IN-SITU MEASUREMENTS

A number of authors have demonstrated the influence of chlorophyll content on the shape of water spectra and have utilized these features for remote sensing [Arvesen *et al.*, 1973; Grew, 1973; and Viollier *et al.*, 1978]. Most of these studies link the chlorophyll concentration in the ocean with changes in the upwelling radiation in two wavelength bands: one in the 450–500 nm region and the other in the green region between 525–540 nm. Recently, the successful extraction of chlorophyll information from spectral bands near 685 nm and 662 nm have been reported [Neville and Gower, 1977 and Wilson *et al.*, 1978].

Two sets of U2-OCS data have provided opportunities to verify the ability of the described analysis technique to detect variations in chlorophyll content in deep ocean water. The first of these data sets was obtained during a Monterey Bay Biology Study Experiment which was conducted jointly by Oregon State University, the U.S. Naval Post-Graduate School and NASA/GSFC teams. The second data set was obtained from a U2-OCS flight in support of a pre-Georgia Bight Experiment (GABEX) cruise. This experiment was conducted in the Atlantic coastal waters near Jacksonville, Florida by L. Atkinson (Skidaway Institute of Oceanography) and associates from Skidaway, the University of Miami and North Carolina State University.

The analysis technique consisted of first determining the ocean spectral radiance from OCS data by applying a correction to eliminate the obscuring effects of the atmosphere. This involved the use of equations 1–4. After the ocean radiance was obtained for two OCS channel wavelengths, 472 nm and 548 nm, the following ratio was calculated

$$R = \frac{I^{\text{Water}}_{472\text{ nm}} - I^{\text{Water}}_{548\text{ nm}}}{I^{\text{Water}}_{472\text{ nm}} + I^{\text{Water}}_{548\text{ nm}}}$$

The ratio, R, is referred to as the chlorophyll index. These particular spectral bands were chosen because, as indicated in Figure 5, light at 472 nm is highly affected by chlorophyll absorption while light at 548 nm is minimally affected. The chlorophyll index was calculated on a pixel by pixel basis for selected scenes derived from OCS data from the two experiments mentioned above. Computer produced images of the chlorophyll index from these scenes were made and recorded on photographic film. These images represented areal maps of the chlorophyll gradients within the boundaries of the scenes in Figure 6 and Figure 7. Areas of relatively high chlorophyll concentration were represented by darker areas on the photograph while low concentration was represented by lighter areas. Figure 6 is an image of chlorophyll index produced from the Monterey Experiment. Comparison of the chlorophyll index, R, with the chlorophyll concentration, C, measured by a surface vessel at the 11 points shown on the image, indicates, as expected, a distinct negative relationship between the R and C. On the left of the scene, the flow of the California Current which is low in bio-productivity, is made evident by the light shade of the ocean. This data set was the first in which it was possible to confirm the validity of the described concept of chlorophyll analysis [Zaneveld, 1978].

The second opportunity for validation was provided by the recent Florida overflight. In a carefully designed procedure, the U2 was flown in three parallel and two skew lines covering an area of high chlorophyll concentration. This chlorophyll feature, as monitored by the R/V Gillis, covered an elongated area, greater than 100 km in length, located on the western edge of the Gulf Stream. A composite image of the chlorophyll index was made from the three parallel flight lines and is displayed in Figure 7. This composite clearly shows the distinct upwelling feature extending from top to bottom on the image. The feature separates the shelf water on the left from the infertile Gulf Stream on the right. Flight line E was approximately 18° to the solar plane and was coincident with R/V Gillis track as it proceeded from the Gulf Stream over the chlorophyll maximum to the shelf. A trace of the concentration as measured by the ship is shown in Figure 8B. Above this trace, in Figure 8A, is the trace of the chlorophyll index, R, derived from the OCS as it covered the same course as

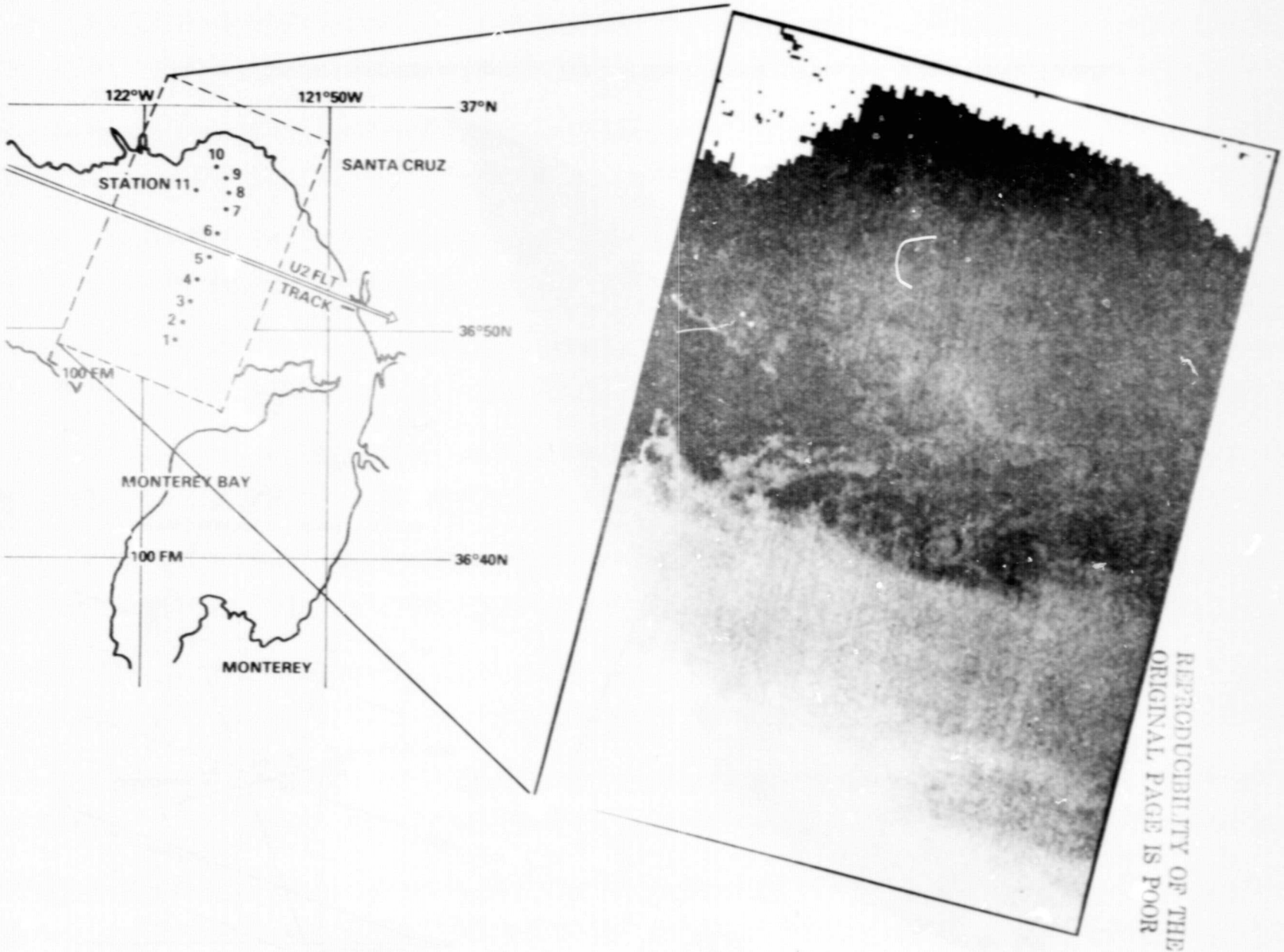




Figure 6. A Composite of Ancillary Map and Computer Enhanced Chlorophyll Gradient Image of the Dotted Area off the Coast of Monterey Bay, California.

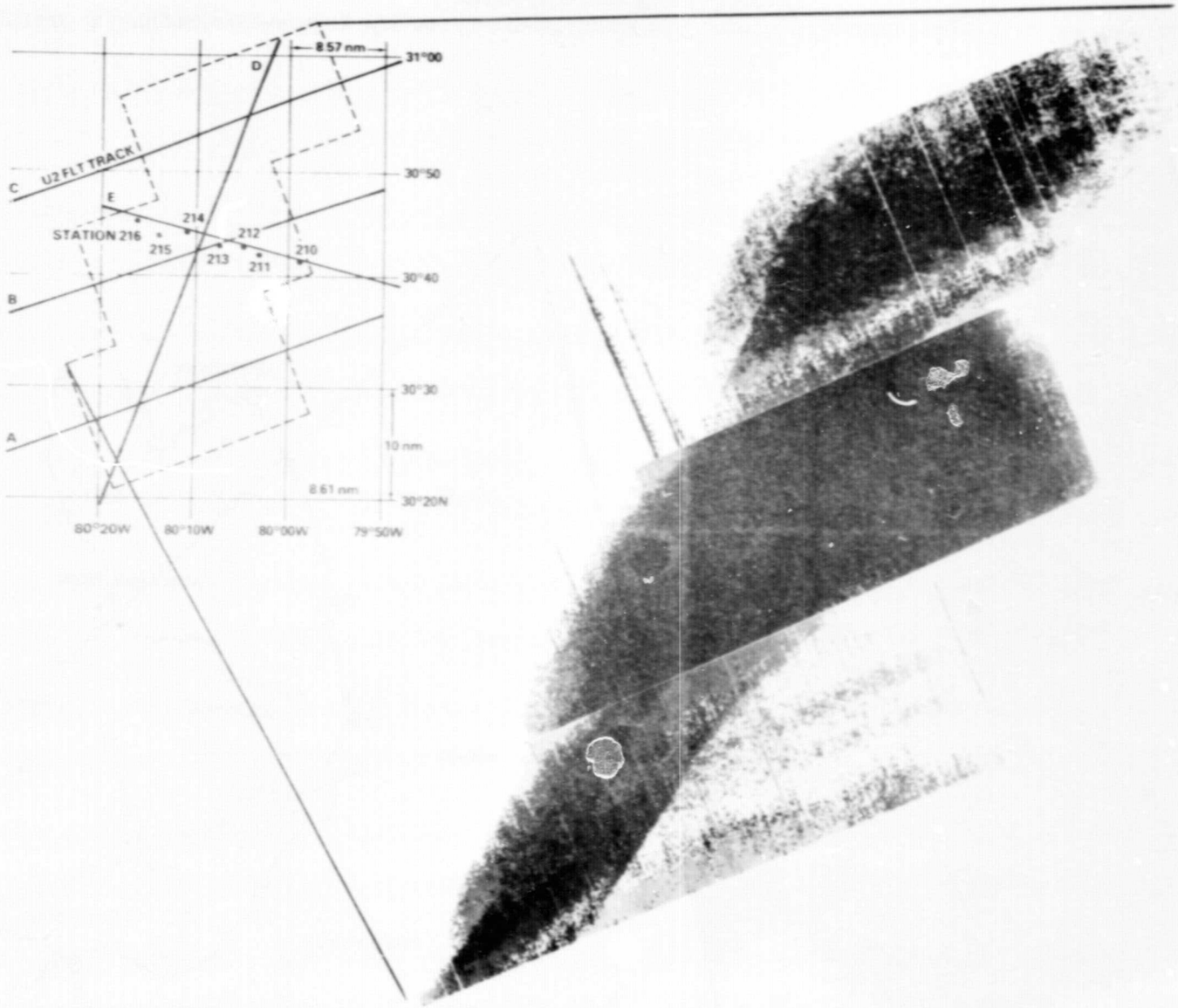


Figure 7. Similar Composite as Figure 6. The Test Site Is About 100 km East of Jacksonville, Florida.

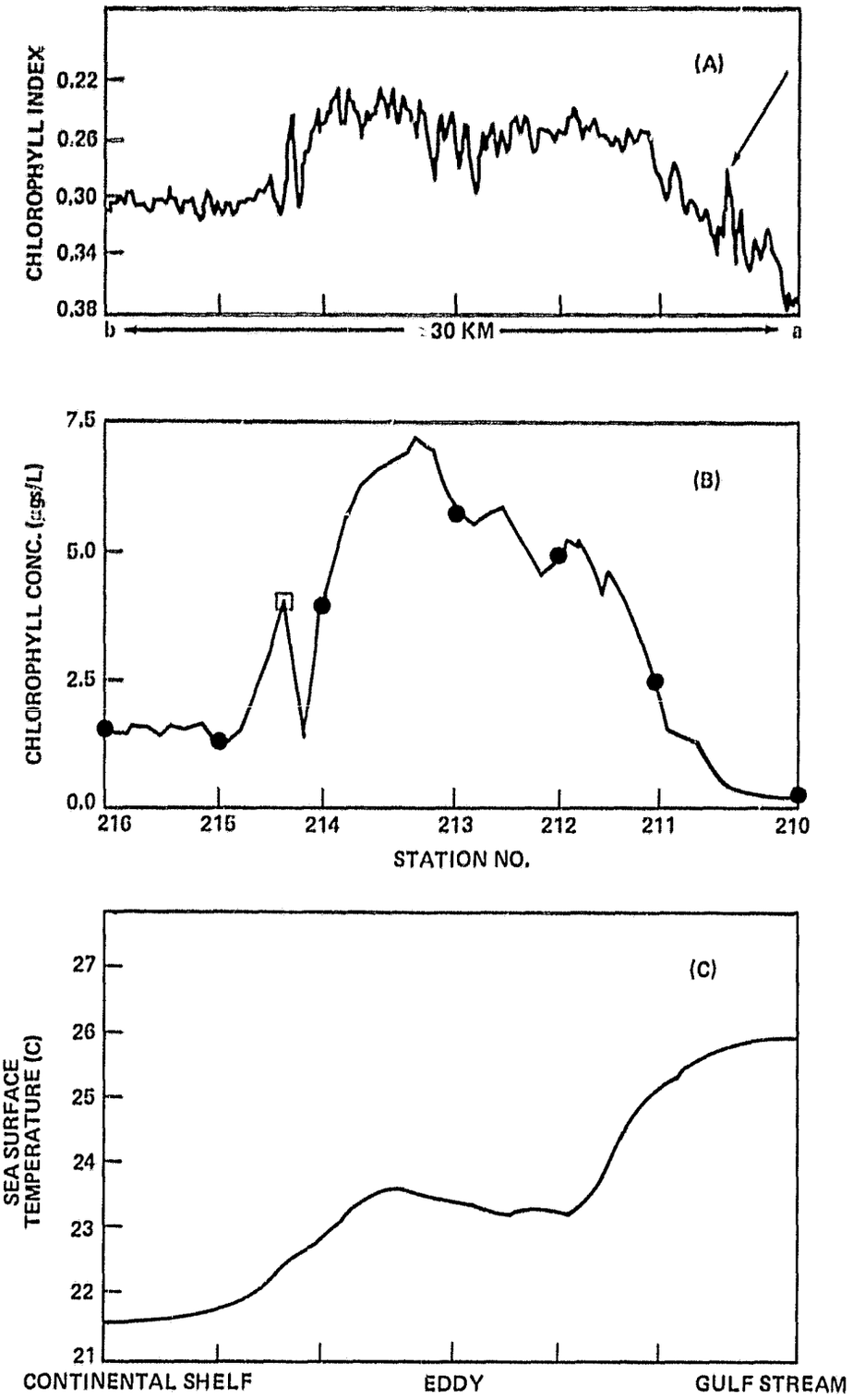


Figure 8. Chlorophyll Index Derived from OCS Data (8A) and a Trace of the Chlorophyll Concentration and Surface Sea Temperature as Measured by the Ship (8B and C) Over the Shiptrack E. The Numbers Along the Bottom of B Indicate Ship Station Numbers. Sighting of the R/V Gillis Is Shown in Arrow in 8A.

the ship by two to three hours prior to the ship's transect. The numbers along the bottom of Figure 8B indicate ship stations where the location of the ship and chlorophyll concentration are precisely known. The two traces show good agreement in the location where the concentration is low or moderate; that is, where the chlorophyll concentration is below about 10 μgs/L. At concentrations above this amount, the index loses sensitivity. Absorption of the blue light by the chlorophyll pigment varies as an inverse exponential of the concentration and thus as the concentration becomes larger, variation of absorption becomes less sensitive to variation of concentration. Hence the peak in concentration as detected by the ship is not clearly distinguishable in the trace of the index.

On the other hand, a sharp minor peak in the chlorophyll concentration between stations 214 and 215 is very distinctly seen in the trace of R. A point of interest is the peak in the trace of R between stations 210 and 211. This peak is an anomaly which resulted when the U2 had the research ship in its view. This fortuitous sighting permitted accurate mapping of the ship track on the OCS image. Figure 8C shows the change in sea surface temperature along the track indicating a rather weak thermal signature. In order to provide an idea of the vertical chlorophyll distribution, Figure 9 is shown. It indicates a large subsurface peak 15-25 meters down, but the top 15 meters is quite uniform.

A plot was made of the chlorophyll concentration C and the chlorophyll index R for the seven station locations from the Atlantic experiment, in triangles, and five deep water spots from the Pacific Ocean, in crosses. This plot is shown in Figure 10. A least squares method was used to fit the data with a line of the following form:

$$C = ae^{bR}$$

The coefficients a and b were determined to be 801 μgs/L and 20.8, respectively. The correlation coefficient for the points in ℓn (C) versus R was -0.965. It would be desirable to establish a universal quantitative relationship between the chlorophyll concentration, C, and R, or some other parameter produced from remote sensed data. This would require repeated field experiments so that a library of data could be developed.

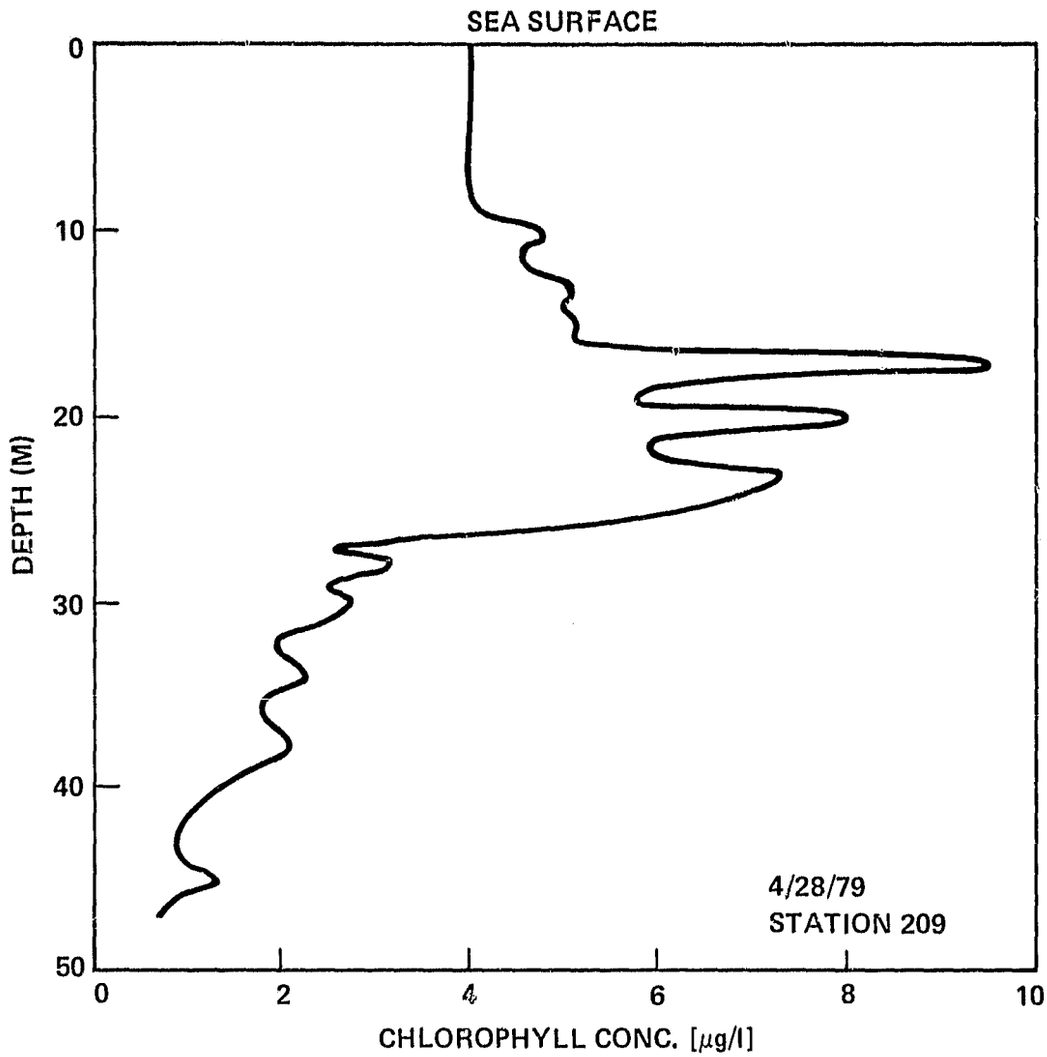


Figure 9. Vertical Distribution of Chlorophyll at Gillis Station 209 Just South of Transect E.

## CONCLUSIONS

The preceding sections summarize recent progress in the development of ocean colorimetric techniques for detecting ocean chlorophyll. It is believed that some significant gains have been achieved in constructing ocean chlorophyll gradient maps which closely match surface truth. The method used to remove the effects of the earth's atmosphere should also be useful in processing similar satellite imagery since the raw data was collected from a U-2 aircraft flying at 19.8 km altitude where approximately 95% of the total atmosphere is included.

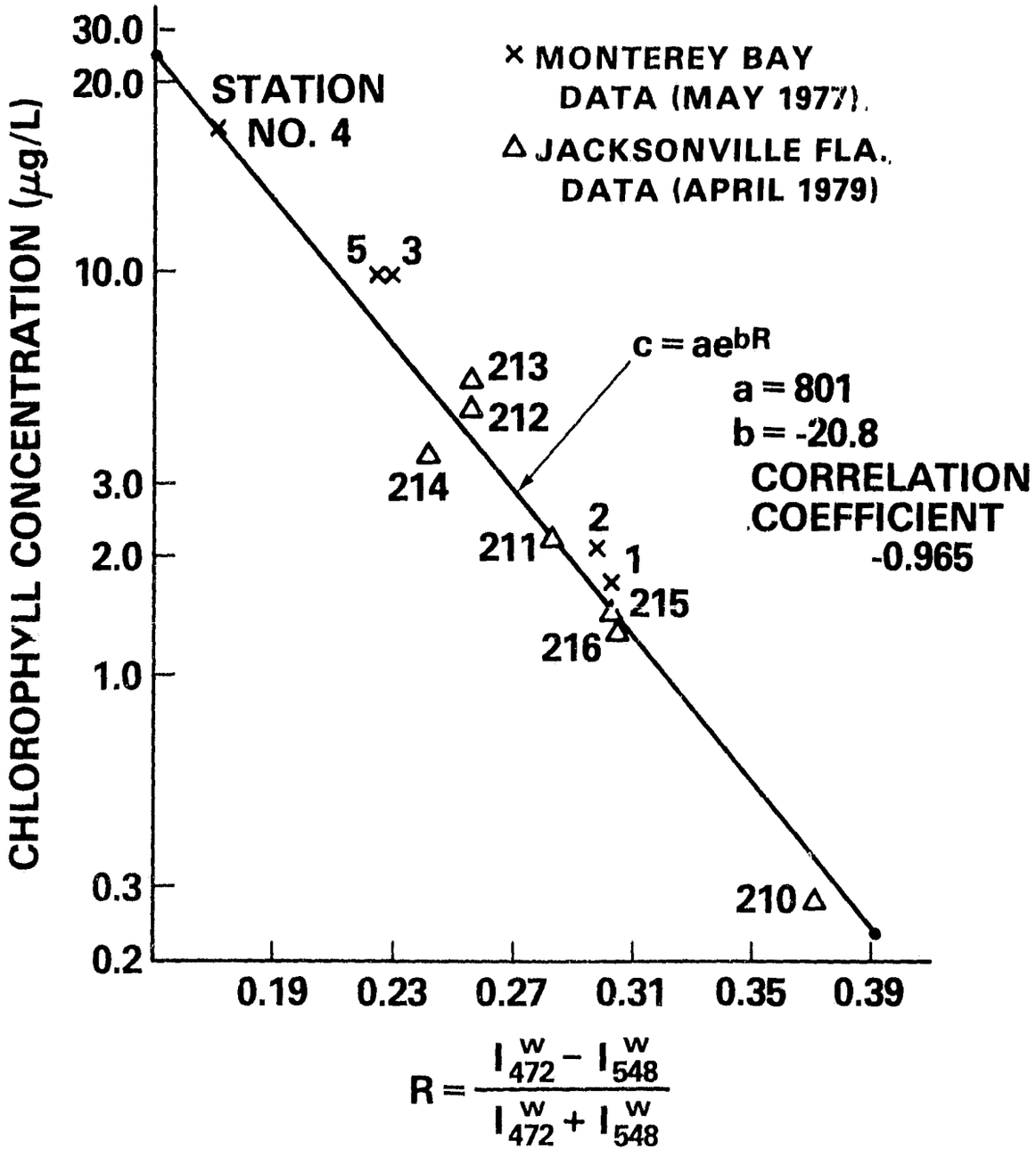


Figure 10. Correlation Between the Measured Chlorophyll Concentration, C, and Derived Products, R, by Taking the Ratio of $I_{472\ nm}$ and $I_{548\ nm}$ is Shown. The Calculated Correlation Coefficient for the Points Was -0.965.

Earlier efforts to use U-2/OCS data have been hampered by the fact that the data was generally obtained in coastal regions. Coastal color phenomenology is extremely complex and multifaceted. The utilization of the analysis technique that has been described could not be demonstrated in a specific application due to the lack of a reliable underwater radiative transfer process modeling method which could deal with the light scattering properties of hydrosols. For these reasons, the authors have limited the scope of this study to conditions of clear water in open ocean areas. The results of the study confirm the validity of the approach.

Thus far, the results of the study indicate that the application of this colorimetric technique for bio-resources remote sensing is well suited to open ocean studies. As exhibited in the correlation plot of Figure 10, chlorophyll measurement is easiest when concentrations are in the low $\mu$g/L range. This is because the upwelling radiance changes due to the chlorophyll concentration is an exponential function and the quantizing range of the instrument will determine the upper limits of resolvable chlorophyll concentration. The data shows that the chlorophyll concentration can be determined up the 10 $\mu$g/L level with reasonable accuracy and reliability. Chlorophyll distribution patterns in the open ocean are an important indication of changes in water type which reflect the circulation and anomalies associated with the main flow, such as regional upwelling phenomena, or meandering eddies. The subtle differences in chlorophyll content in large water bodies of different origins can be recognized by this ocean colorimetric technique. For these reasons it is desirable that further study be conducted to obtain more comprehensive data sets so that the analysis algorithms can be further improved.

## ACKNOWLEDGMENTS

The authors wish to thank R. S. Fraser for helpful discussions concerning the atmospheric radiance.

## REFERENCES

Arveson, J. C., J. P. Millard, and E. C. Weaver, Remote sensing of chlorophyll and temperature in marine and fresh waters, Astronaut. Acta., 18, 229-239, 1973.

Bahethi, O. P., R. S. Fraser, Effect of molecular anisotropy on the intensity and degree of polarization of light scattered from model atmospheres, NASA-GSFC X document 910-75-52, 1975.

Clark, G. L., G. C. Ewing and C. J. Lorenzen, Spectra of backscattered light from the sea obtained from aircraft as measure of chlorophyll concentration, Science, 167, 1119-20, 1970.

Cox, C. and W. Munk, Slopes of the sea surface deduced from photographs of sun glitter, Bull. Scripps Inst. of Ocean., 6, 401-488, 1956.

Dave, J. W., Development of programs for computing characteristics of ultraviolet radiation, Tech-report-Scalar Case (SPA-D) NASA Contract 5-2168 Report, IBM, 1972.

Gordon, H., Removal of atmospheric effects from satellite imagery of the oceans, Applied Optics, 17, 1631-5, 1978.

Grew, G. W., Signature analysis of reflectance spectra of phytoplankton and sediment in inland waters, Remote Sensing of Earth Resources, 2, 1147-72, Univ. of Tennessee, 1973.

Hovis, W. A., M. L. Forman, and L. R. Blaine, Detection of ocean color changes from high altitude, NASA-GSFC X-document 652-73-371, 1973.

Kattawar, G. W. and T. J. Humphreys, Remote sensing of chlorophyll in an atmosphere-ocean environment; a theoretical study, Applied Optics, 15, 273-82, 1976.

Kim, H. H., R. S. Fraser, L. Thompson, and O. P. Bahethi, A system study of an advanced ocean color scanner, Boundary Layer Meteorology, to be published in 1979.

Neville, R. A., and J. F. R. Gower, Passive remote sensing of phytoplankton via chlorophyll fluorescence, J. G. R., 82, 3487-93, 1977.

Plass, G. N., G. W. Kattawar and J. A. Guinn, Jr., Radiance distribution over a ruffled sea; contributions from glitter, sky and ocean, Applied Optics, 15, 3161-65, 1976.

Quenzel, H. and M. Kästner, Masking effects by the atmosphere on remote sensing of chlorophyll in the ocean. Final Report, Univ. of München, 1978.

Sumphner, W. E., Physical Soc. Proc., 12, 10, 1892.

Thekaekara, M. P., Extraterrestrial solar spectrum, 3000 – 6000 Å at 1 Å intervals, Applied Optics, 13, 518-22, 1974.

Viollier, M., P. Y. Deschamps, and P. Lecomte, Airborne remote sensing of chlorophyll content under cloudy sky as applied to the tropical water in the Gulf of Guinea, Remote Sensing of Environment, Elsevier, 7, 187-202, 1978.

Wilson, W. H., R. W. Austin and R. C. Smith, Optical remote sensing of chlorophyll in ocean waters, Proc. of 12th Int. Symposium on Remote Sensing of Environment, ERIM, 1103-1113, 1978.

Zaneveld, J. R., J. C. Kitchen, R. Barts, D. Menzies, S. Moore, R. Spinrod, and H. Pak, NASA-Contract S-23728 Report, Oregon State Univ. School of Oceanography, 1978.

## APPENDIX A

The effect of OCS's polarization sensitivity to the sky polarization can be estimated in the following manner.

$$\begin{vmatrix} I_l \\ I_r \end{vmatrix} = \begin{vmatrix} t_l t_{lr} \\ t_{rl} t_r \end{vmatrix} \begin{vmatrix} I_l^\circ \\ I_r^\circ \end{vmatrix} \tag{1A}$$

where $I_l^\circ$ and $I_r^\circ$ are the intensities of the orthogonal components of the incident light, $I_l$ and $I_r$ are the intensities measured by OCS and $t_l$, $t_{lr}$, $t_r$, $t_{rl}$ are radiative transfer matrix elements characterizing the instruments. For OCS, $t_l$ and $t_r$ were 1.0 and 0.8 respectively and $t_{lr}$ and $t_{rl}$ were zero. The components, $I_l^\circ$ and $I_r^\circ$, are computed by using a modified Dave program in which polarization characteristics of the radiation are taken into account. In the cases where the OCS was flown either directly away or toward the sun while maintaining a solar zenith angle of 45°, the scanner's ±45° scan is orthogonal to the solar radiance plane. This scanning motion will not cause a change in polarization direction, but will cause a fluctuation in total intensity.

The calculated normalized intensities of components $I_l^\circ$ and $I_r^\circ$ at 548 nm for a 1% ground reflectivity are given in the following table.

| Scan Angle | $I_l^\circ$ | $I_r^\circ$ |
|---|---|---|
| 0° | 0.623 | 0.373 |
| ±45° | 0.576 | 0.424 |

From equation 1A, the total intensities perceived by the instrument at 0° and ±45° scan angles are 0.9245 and 0.9151 respectively. The error in $I_{total}$ that is introduced by the instrument is:

$$\% \text{ error} = \frac{0.9245 - 0.9151}{0.9245} \times 100 = 1.01\%$$

## APPENDIX B

The technical report for the scalar case which was developed for NASA by J. V. Dave in 1972 pertains to the basic transfer equation for a plane parallel atmosphere which has the following forms:

$$\mu \frac{dI(\tau; \mu\varphi)}{d\tau} = I(\tau: \mu, \varphi) - \omega(\tau)\, J(\tau: \mu, \varphi)$$

Where $\mu, \varphi$ are directional parameters and $\tau$ refers to optical depth. $\omega(\tau)$ is the single scattering albedo and J, the source function is given by

$$J(\tau: \mu, \varphi) = \tfrac{1}{4}Fe^{-\tau/\mu_0}\, P(\tau: \mu, \varphi: -\mu_0, \varphi_0) + \tfrac{1}{4\pi}\int_{-1}^{+1}\int_{0}^{2\pi} P(\tau: \mu, \varphi; \mu', \varphi')\, I(\tau: \mu', \varphi')\, d\mu' d\varphi'$$

F denotes for the solar flux and $P(\tau: \mu, \varphi; \mu', \varphi')$ is the normalized scattering phase function. This quantity represents the fraction of incident energy scattered by a unit volume at $\tau$ and includes the contribution of Mie and Rayleigh scattering.

Detailed aspects of these computation programs are divided into 4 part reports (NAS-5-21680). The purpose of the Fortran programs are for computing the intensity of the scattered radiation emerging at any level of a plane parallel, non-homogeneous atmosphere continuing an arbitrary vertical distribution of ozone concentration and an aerosol number density, and bounded at the lower end by a Lambert ground of known reflectivity.

## FIGURE CAPTIONS

Figure 1. A Measurement of Downward Atmospheric Radiance by the Use of U2/OCS, in Triangles, Is Compared with the Calculated Values Given in Dots.

Figure 2. Upwelling Intensity for Each OCS Channel is Plotted Against Aerosol Content Showing Radiance Differences Due To the Aerosol Size Distributions, $\upsilon^* = 3.2$, in Dots, and 3.5, in Triangles. The Calculations Are for Nadir Viewing Normalized to a Solar Zenith Angle of 30° and Ground Reflectivity of 1%.

Figure 3. Plots of Upwelling Radiance at Nine OCS Channels. Bars Are Actual OCS Data Taken From U-2 Flight off the Jacksonville, Florida. The Solid Line Indicates Calculated Radiance of the Atmosphere and Surface Reflection, and the Dotted Line Corresponds to Calculated Radiance which Includes the Radiance Contribution of Ocean Subsurface Layer.

Figure 4. Plots of Clear Ocean Albedo Showing Their Wavelength Dependency. Solid Line Profile Was Used for Our Calculation.

Figure 5. Derived Water Radiance from OCS Data: The Spectral Feature from Low Chlorophyll Concentration Is Shown in Circles and Interconnecting Line. The Triangular Trace Belongs to That of a High Chlorophyll Zone.

Figure 6. A Composite of Ancillary Map and Computer Enhanced Chlorophyll Gradient Image of the Dotted Area off the Coast of Monterey Bay, California.

Figure 7. Similar Composite as Figure 6. The Test Site Is About 100 km East of Jacksonville, Florida.

Figure 8. Chlorophyll Index Derived from OCS Data (8A) and a Trace of the Chlorophyll Concentration and Surface Sea Temperature as Measured by the Ship (8B and C) Over the Ship-track E. The Numbers Along the Bottom of B Indicate Ship Station Numbers. Sighting of the R/V Gillis Is Shown in Arrow in 8A.

Figure 9. Vertical Distribution of Chlorophyll at Gillis Station 209 Just South of Transect E.

Figure 10. Correlation Between the Measured Chlorophyll Concentration, C, and Derived Products, R, by Taking the Ratio of $I_{472\ nm}$ and $I_{548\ nm}$ is Shown. The Calculated Correlation Coefficient for the Points Was -0.965.

## BIBLIOGRAPHIC DATA SHEET

| 1. Report No. 80574 | 2. Government Accession No. | 3. Recipient's Catalog No. |
|---|---|---|
| 4. Title and Subtitle<br>Ocean Chlorophyll Studies From a U-2 Aircraft Platform | | 5. Report Date<br>6. Performing Organization Code |
| 7. Author(s) H. H. Kim, C. R. McClain, L. R. Blaine, W. D. Hart, L. P. Atkinson and J. A. Yoder | | 8. Performing Organization Report No. |
| 9. Performing Organization Name and Address<br>Earth Observations Systems Division<br>Code 940<br>Goddard Space Flight Center<br>Greenbelt, Maryland 20771 | | 10. Work Unit No.<br>11. Contract or Grant No.<br>13. Type of Report and Period Covered<br>Technical Memorandum |
| 12. Sponsoring Agency Name and Address<br>NASA/Goddard Space Flight Center<br>Greenbelt, Maryland 20771 | | 14. Sponsoring Agency Code |
| 15. Supplementary Notes | | |

16. Abstract

Chlorophyll gradient maps of large ocean areas were generated from U2/OCS data obtained over test sites in the Pacific and Atlantic Oceans. The delineation of oceanic features using the upward radiant intensity relies on an analysis method which presupposes that radiation backscattered from the atmosphere and ocean surface can be properly modeled using a measurement made at 778 nm. The calculation of atmospheric radiance was performed using a method developed by J. V. Dave. An estimation of the chlorophyll concentration is performed by properly ratioing radiances measured at 472 nm and 548 nm after removing the atmospheric effects. The correlation between the remotely sensed data and in-situ surface chlorophyll measurements has been validated in two sets of data. The results show that the correlation between the in-situ measured chlorophyll and the derived quantity is a negative exponential function and the correlation coefficient was calculated to be -0.965.

| 17. Key Words (Selected by Author(s)) | 18. Distribution Statement |
|---|---|
| Chlorophyll remote sensing<br>Ocean color | |

| 19. Security Classif. (of this report) | 20. Security Classif. (of this page) | 21. No. of Pages | 22. Price* |
|---|---|---|---|
| Unclassified | Unclassified | | |

*For sale by the National Technical Information Service, Springfield, Virginia 22151.

GSFC 25-44 (10/77)